Peer Community In
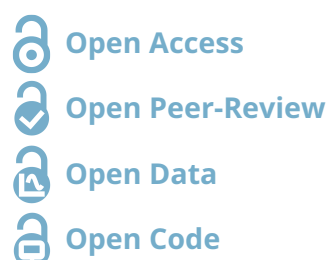## Evolutionary Biology

Quantifying transmission dynamics of acute hepatitis C virus infections in a heterogeneous population using sequence data

Gonché Danesh[1], Victor Virlogeux[2] & Christophe Ramière[3] & Caroline Charre[3] & Laurent Cotte[4] & Samuel Alizon[1]

[1] MIVEGEC, CNRS, IRD, Université de Montpellier – Montpellier, France

[2] Clinical Research Center, Croix-Rousse Hospital, Hospices Civils de Lyon – Lyon, France

[3] Virology Laboratory, Croix-Rousse Hospital, Hospices Civils de Lyon – Lyon, France

[4] Infectious Diseases Department, Croix-Rousse Hospital, Hospices Civils de Lyon – Lyon, France

An article peer-reviewed and recommended by *Peer Community In Evolutionary Biology*, edited by David Rasmussen on the basis of the reviews by Chris Wymant and Louis DuPlessis (DOI: 10.24072/pci.evolbiol.100117)
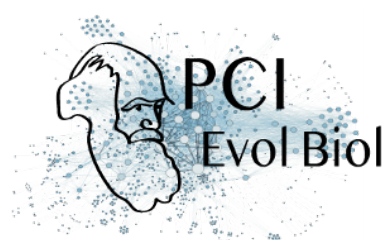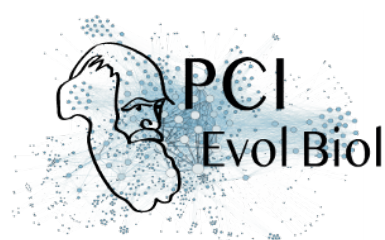
Abstract

Opioid substitution and syringes exchange programs have drastically reduced hepatitis C virus (HCV) spread in France but HCV sexual transmission in men having sex with men (MSM) has recently arisen as a significant public health concern. The fact that the virus is transmitting in a heterogeneous population, with 'new' and 'classical' hosts, makes prevalence and incidence rates poorly informative. However, additional insights can be gained by analyzing virus phylogenies inferred from dated genetic sequence data. By combining a phylodynamics approach based on Approximate Bayesian Computation (ABC) and an original transmission model, we estimate key epidemiological parameters of an ongoing HCV epidemic among MSMs in Lyon (France). We show that this new epidemic is largely independent of the 'classical' HCV epidemics and that its doubling time is ten times lower (0.44 years *versus* 4.37 years). These results have practical implications for HCV control and illustrate the additional information provided by virus genomics in public health.

Keywords: Phylodynamics; Genomics; Hepatitis C virus; Public health; Approximate Bayesian Computation

Background

It is estimated that 71 million people worldwide suffer from chronic hepatitis C virus (HCV) infections (European Union HCV Collaborators, 2017; Messina et al., 2015). The World Health Organisation (WHO) and several countries have issued recommendations towards the 'elimination' of this virus, which they define as an 80% reduction in new chronic infections and a 65% decline in liver mortality by 2030 (European Union HCV Collaborators, 2017). HIV-HCV coinfected patients are targeted with priority because of the shared transmission routes between the two viruses (Alter, 2006) and because of the increased virulence of HCV in coinfections (Klein et al., 2016; Kovari et al., 2015; Rosenthal et al., 2009). Successful harm reduction interventions, such as needle-syringe exchange and opiate substitution programs, as well as a high level of enrolment into care programs for HIV-infected patients, have led to a drastic drop in the prevalence of active HCV infections in HIV-HCV coinfected patients in several European countries during the recent years (Béguelin et al., 2018; Berenguer et al., 2018; Boerekamps et al., 2018; Pradat, Pugliese, et al., 2017). Unfortunately, this elimination goal is challenged by the emergence of HCV sexual transmission, especially among men having sex with men (MSM). This trend is reported to be driven by unprotected sex, drug use in the context of sex ('chemsex'), and potentially traumatic practices such as fisting (T vd Laar et al., 2009; Pradat, Huleux, et al., 2018; Salazar-Vizcaya et al., 2016). The epidemiology of HCV infection in the Dat'AIDS cohort has been extensively described from 2000 to 2016 (D'Oliveira et al., 2005; Pradat, Caillat-Vallet, et al., 2001; Sahajian et al., 2011). The incidence of acute

HCV infection has been estimated among HIV-infected MSM between 2012 and 2016, among HIV-negative MSM enrolled in PrEP between in 2016-2017 (Pradat, Huleux, et al., 2018) and among HIV-infected and HIV-negative MSMs from 2014 to 2017 (Ramière et al., 2019). In the area of Lyon (France), HCV incidence has been shown to increase concomitantly with a shift in the profile of infected hosts (Ramière et al., 2019). Understanding and quantifying this recent increase is the main goal of this study.

Several modelling studies have highlighted the difficulty to control the spread of HCV infections in HIV-infected MSMs in the absence of harm reduction interventions (Salazar-Vizcaya et al., 2016; Virlogeux et al., 2017). Furthermore, we recently described the spread of HCV from HIV-infected to HIV-negative MSMs, using HIV pre-exposure prophylaxis (PrEP) or not, through shared high-risk practices (Ramière et al., 2019). More generally, an alarming incidence of acute HCV infections in both HIV-infected and PrEP-using MSMs was reported in France in 2016-2017 (Pradat, Huleux, et al., 2018). Additionally, while PrEP-using MSMs are regularly screened for HCV, those who are HIV-negative and do not use PrEP may remain undiagnosed and untreated for years. In general, we know little about the population size and practices of HIV-negative MSM who do not use PrEP. All these epidemiological events could jeopardize the goal of HCV elimination by creating a large pool of infected and undiagnosed patients, which could fuel new infections in intersecting populations. Furthermore, the epidemiological dynamics of HCV infection have mostly been studied in intravenous drug users (IDU) (Kwon et al., 2009; Pitcher et al., 2018; Pybus, Cochrane, et al., 2005; Sweeting et al., 2008) and the general population (Breban et al., 2014; Heffernan et al., 2019). Results from these populations are not easily transferable to other populations, which calls for a better understanding of the epidemiological characteristics of HCV sexual transmission in MSM.

Given the lack of knowledge about the focal population driving the increase in HCV incidence, we analyse virus sequence data with phylodynamics methods. This research field has been blooming over the last decade and hypothesizes that the way rapidly evolving viruses spread leaves 'footprints' in their genomes (Frost et al., 2015; Grenfell et al., 2004; Volz, Koelle, et al., 2013). By combining mathematical modelling, statistical analyses and phylogenies of infections, where each leaf corresponds to the virus sequence isolated from a patient, current methods can infer key parameters of viral epidemics. This framework has been successfully applied to other HCV epidemics (Joy et al., 2016; Magiorkinis et al., 2009; Pybus, Charleston, et al., 2001; Stadler et al., 2013), but the ongoing one in Lyon is challenging to analyze because the focal population is heterogeneous, with 'classical' hosts (typically HIV-negative patients infected through nosocomial transmission or with a history of opioid intravenous drug use or blood transfusion) and 'new' hosts (both HIV-infected and HIV-negative MSM, detected during or shortly after acute HCV infection phase, potentially using recreational drugs such as cocaine or cathinones), where host profiles have been established by field epidemiologists based on interviews and risk factors. Our phylodynamics analysis relies on an Approximate

Bayesian Computation (ABC, (Beaumont et al., 2002)) framework that was recently developed and validated using a simple Susceptible-Infected-Recovered (SIR) model (Saulnier et al., 2017).

Assuming an epidemiological transmission model with two host types, 'classical' and 'new' (see the Methods), we use dated virus sequences to estimate the date of onset of the HCV epidemics in 'classical' and 'new' hosts, the level of mixing between hosts types, and, for each host type, the duration of the infectious period and the effective reproduction ratio (i.e. the number of secondary infections, (Anderson and May, 1991)). To validate our results we performed a parametric bootstrap analysis, we tested the sensitivity of the method to differences in sampling proportions between the two types of hosts. We also tested the sensitivity of the method to phylogenetic reconstruction uncertainty, and we performed a cross-validation analysis to explore the robustness of our inference framework. We find that the doubling time of the epidemics is one order of magnitude lower in 'new' than in 'classical' hosts, therefore emphasising the urgent need for public health action.

Results

The phylogeny inferred from the dated virus sequences shows that 'new' hosts (in red) tend to be grouped in clades (Figure 1). This pattern suggests a high degree of assortativity in the epidemics (i.e. hosts tends to infect hosts from the same type). The ABC phylodynamics approach allows us to go beyond a visual description and to quantify several epidemiological parameters.

As for any Bayesian inference method, we need to assume a prior distribution for each parameter. These priors, shown in grey in Figure 2, are voluntarily designed to be large and uniformly distributed to be as little informative as possible. One exception is the date of onset of the epidemics, for which we use the output of the phylogenetic analysis conducted in Beast (see the Methods) as a prior. We also assume the date of the 'new' hosts epidemics to be after 1997 based on epidemiological data.

The inference method converges towards posterior distributions for each parameter, which are shown in red in Figure 2. The estimate for the origin of the epidemic in 'classical' hosts is $t_0 = 1957.47\,[1948.61; 1961.96]$ (numbers in brackets indicate the 95% Highest Posterior Density, or HPD). For the 'new' host type, we were not able to estimate when the epidemic (t_2) has started.

We find the level of assortativity between host types to be high for 'classical' ($a_1 = 0.94\,[0.83; 1.0]$) as well as for 'new' hosts ($a_2 = 0.92\,[0.81; 0.99]$). Therefore, hosts mainly infect hosts from the same type.

The phylodynamics approach also allows us to infer the duration of the infectious period for each host type. Assuming that this parameter does not vary over time, we estimate it to
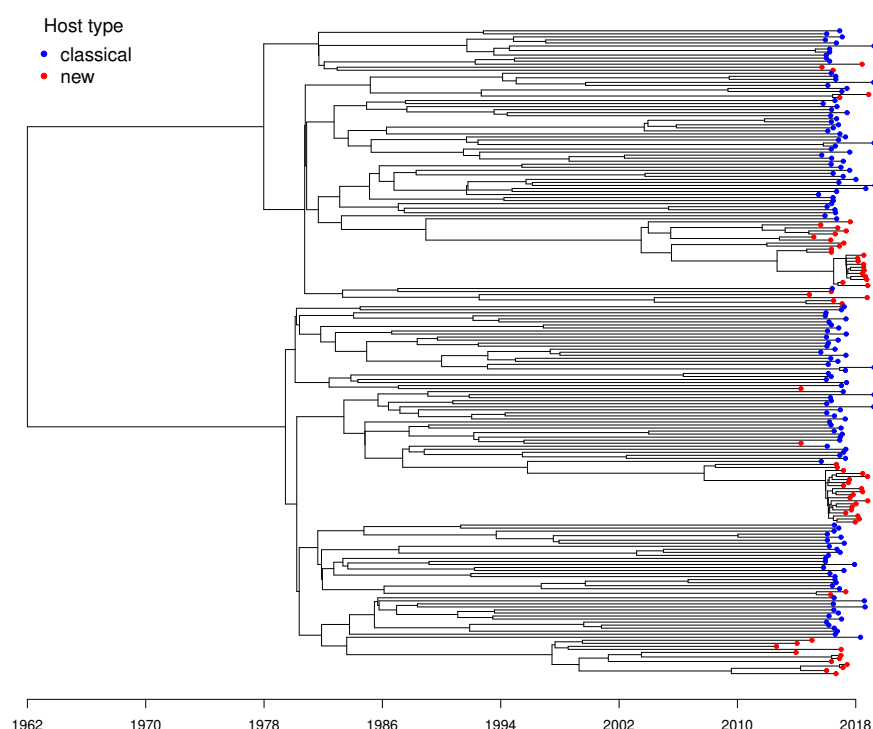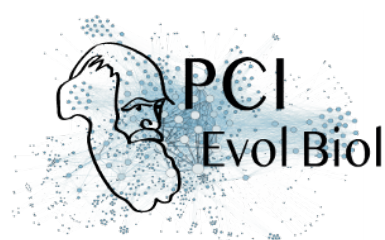
Figure 1. Phylogeny of HCV infections in the area of Lyon (France). 'Classical' hosts are in blue and 'new' hosts are in red. Sampling events correspond to the end of black branches. The phylogeny was estimated using Bayesian inference (Beast2). See the Methods for additional details.

be 3.85 years $[1.09; 8.33]$ for 'classical' hosts (parameter $1/\gamma_1$) and 0.45 years $[0.30; 0.77]$ for 'new' hosts (parameter $1/\gamma_2$). We compute the ratio of γ_2/γ_1 and the 95% credibility interval does exclude 1.

Regarding effective reproduction numbers, i.e. the number of secondary infections caused by a given host over its infectious period, we estimate that of 'classical' hosts to have decreased from $R^{(1),t_1} = 1.96\ [1.45; 3.29]$ to $R^{(1),t_2} = 1.61\ [1.05; 2.08]$ after the introduction of the third-generation HCV test in 1997. The inference on the differential transmission parameter indicates that HCV transmission rate is $\nu = 9.0\ [7.7; 9.9]$ times greater from 'new' hosts than from 'classical' hosts. By combining these results (see the Methods), we compute the effective reproduction number in 'new' hosts and find $R^{(2),t_3} = 1.73\ [1.03; 4.32]$. We compute the ratio of the $R(t)$ of 'new' hosts over the $R(t)$ of 'classical' hosts after 1997 and,
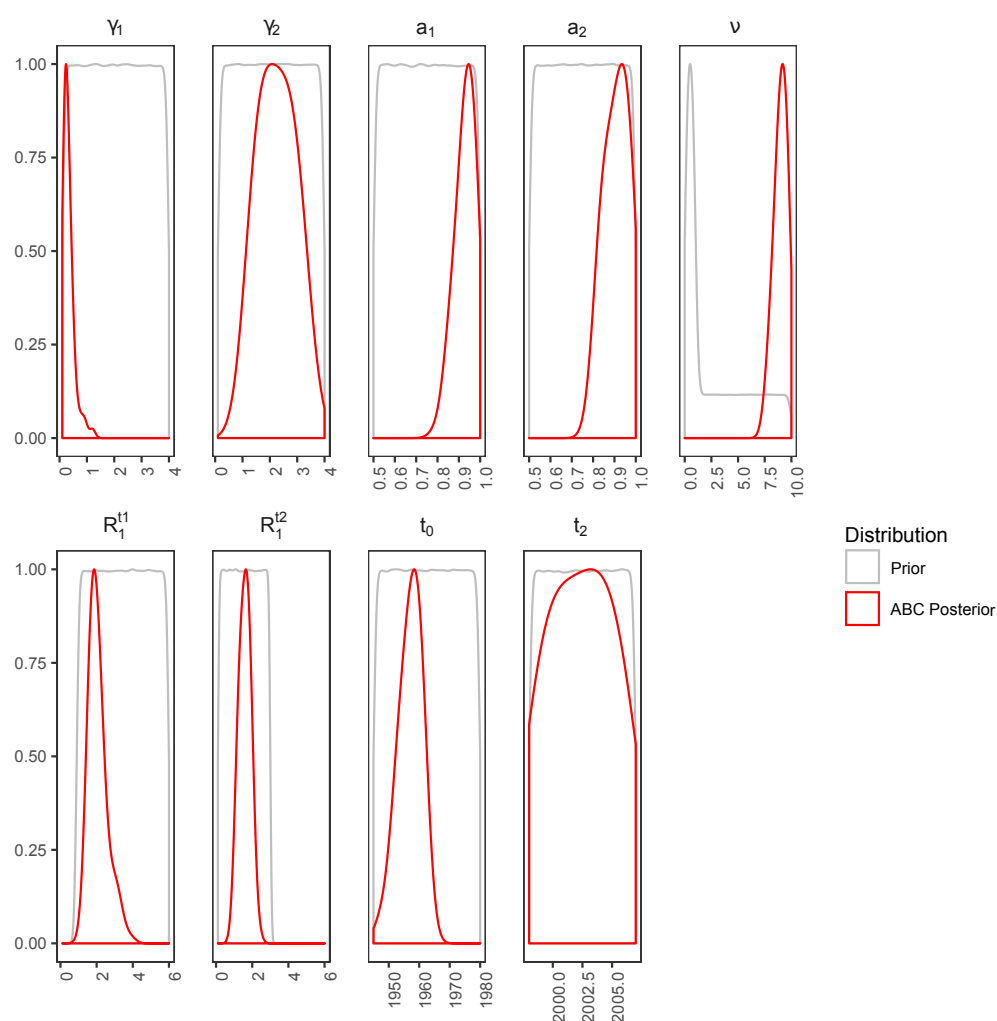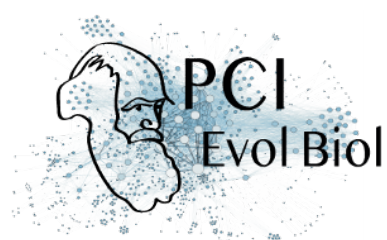
Figure 2. Parameter prior and posterior distributions. Prior distributions are in grey and posterior distributions inferred by ABC are in red. The thinner the posterior distribution width, the more accurate the inference. Posterior distributions are truncated based on the prior distribution.

the median value is 1.14 and the 95% credibility interval is $[0.56; 3.25]$.

To better understand the differences between the two host types, we compute the epidemic doubling time (t_D), which is the time for an infected population to double in size. t_D is computed for each type of host, assuming complete assortativity (see the Methods). We find that for the 'classical' hosts, before 1997 $t_D^{(1),t1} \approx 2.8$ years ($[1.1; 5.0]$ years). After 1997, the pace decreases with a doubling time of $t_D^{(1),t2} \approx 4.4$ years ($[2.0; 20.8]$ years). For the epidemics in the 'new' hosts, we estimate that $t_D^{(2),t3} \approx 0.44$ years ($[0.09; 8.84]$ years). When computing the ratio of the doubling times of classical hosts after 1997 over the doubling times of the new
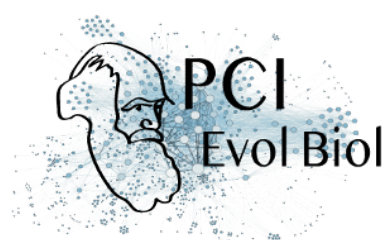
hosts ($t_D^{(1),t2}/t_D^{(2),t3}$) to estimate the current difference we find that $t_D^{(1),t2}$ is 10 times higher than $t_D^{(2),t3}$ with a 95% credibility interval of $[0.62; 149.99]$. However, the 75% credibility interval does exclude 1 and is $[3.39; 25.61]$. Distributions for theses three doubling times are shown in Supplementary Figure S2.

Supplementary Figure S3 shows the correlations between parameters based on the posterior distributions. We mainly find that the R_t in 'classical' hosts after the introduction of the third generation of HCV detection tests (i.e. $R^{(1),t_2}$) is negatively correlated to ν and positively correlated to γ_2. In other words, if the epidemic spreads rapidly in 'classical' hosts, it requires a slower spread in 'new' hosts to explain the phylogeny. $R_0^{(1),t_2}$ is also slightly negatively correlated to γ_1, which most likely comes from the fact that for a given R_0, epidemics with a longer infection duration have a lower doubling time and therefore a weaker epidemiological impact. Overall, these correlations do not affect our main results, especially the pronounced difference in infection periods (γ_1 and γ_2).

To validate these results, we performed a goodness-of-fit test by simulating phylogenies using the resulting posterior distributions to determine whether these are similar to the target dataset (see the Methods). In Figure 3, we see that the target data in red, i.e. the projection of the observed summary statistics from the phylogeny shown in Figure 1, is contained in the envelope containing 90% of the simulations drawn from the posterior distributions. If we use the 95% HPD of the posterior but assume a uniform distribution instead of the true posterior distribution, we find that the target phylogeny is not contained in the envelope. These results confirm that the posterior distributions we infer are highly informative. In Supplementary Figure S4 we show that for 77 summary statistics out of 101, the target value is in the 95% highest posterior distribution of summary statistics computed from the 10,000 simulated phylogenies from the posterior distribution used for the goodness-of-fit test.

To further explore the robustness of our inference method, we use simulated data to perform a 'leave one out' cross-validation (see the Methods). As shown in Supplementary Figure S5, the mean relative error made for each parameter inference is limited and comparable to what was found using a simpler SIR model (Saulnier et al., 2017). One exception is for the 'new' hosts' level of assortativity (a_2). This is likely due to the poor signal given the small size of the observed phylogeny.

A potential issue is that the sampling rate of 'new' hosts may be higher than that of 'classical' hosts. To explore the effect of such sampling biases on the accuracy of our results, we sub-sampled the 'new' hosts population by pruning the target phylogeny, i.e. randomly removing 50% of the 'new' hosts' tips. In Supplementary Figure S6 we show the posterior distributions estimated by our ABC method using the different pruned phylogenies. We find that although the confidence intervals are wider, the posterior distributions are all similar with the posterior distributions estimated using the target phylogeny. Finally, to evaluate the impact of phylogenetic reconstruction uncertainty, we analysed 100 additional trees from the Beast posterior distribution. In Supplementary figure S7, we show that the estimates from our ABC method are qualitatively similar for all these trees.
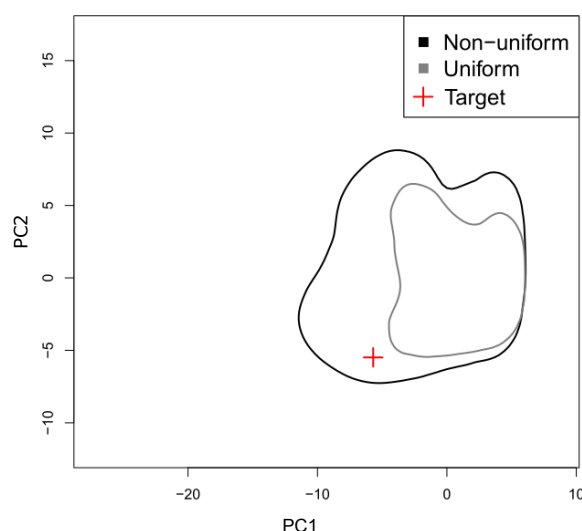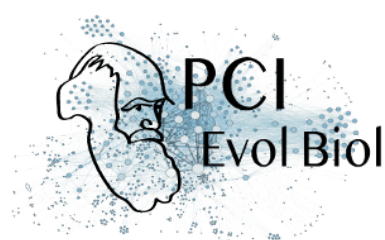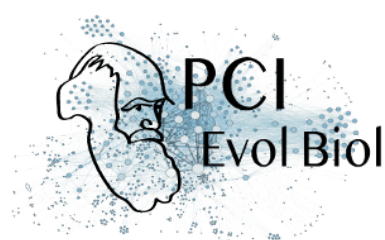
Figure 3. Goodness-of-fit estimated using parameter bootstrap. The graph displays envelopes containing 90% of the $10,000$ simulations for each distribution. The envelope in black results from the posterior distribution, in grey, results from the uniform distribution drawn from the 95% HPD distribution. The target data is represented by a red cross. Axes units are based on the outcome of principal component analysis using the simulated summary statistics.

Discussion

Over the last years, the area of Lyon (France) witnessed an increase in HCV incidence both in HIV-positive and HIV-negative populations of men having sex with men (MSM)(Ramière et al., 2019). This increase appears to be driven by sexual transmission and echoes similar trends in Amsterdam (TJW vd Laar et al., 2007) and Switzerland (Wandeler et al., 2012). A quantitative analysis of the epidemic is necessary to optimise public health interventions. Unfortunately, this is challenging because the monitoring of the population at risk is limited and because classical tools in quantitative epidemiology, especially incidence time series, are poorly informative with such a heterogeneous population. To circumvent this problem, we used HCV sequence data, which we analysed using phylodynamics. To account for host heterogeneity, we extended and validated an existing Approximate Bayesian Computation framework (Saulnier et al., 2017).

From a public health point of view, our results have two major implications. First, we find a strong degree of assortativity in both 'classical' and 'new' host populations. The virus phylogeny does hint at this result (Figure 1) but the ABC approach allows us to quantify the pat-

tern and to show that assortativity may be higher for 'classical' hosts. The second main result has to do with the striking difference in doubling times. Indeed, the current spread of the epidemics in 'new' hosts appears to be five times more rapid than the spread in the 'classical' hosts in the early 1990s before the advent of the third generation tests in 1997, and ten times more rapid that the spread in the 'new' hosts after 1997. That the duration of the infectious period in 'new' hosts is in the same order of magnitude as the time until treatment suggests that the majority of the transmission events may be occurring during the acute phase. This underlines the necessity to act rapidly upon detection, for instance by emphasising the importance of protection measures such as condom use and by initiating treatment even during the acute phase (AASLD/IDSA HCV Guidance Panel, 2015). A better understanding of the underlying contact networks could provide additional information regarding the structure of the epidemics and, with that respect, next-generation sequence (NGS) data could be particularly informative (Romero-Severson et al., 2016; Worby et al., 2017; Wymant et al., 2018).

Some potential limitations of the study are related to the sampling scheme, the assessment of the host type, and the transmission model. Regarding the sampling, the proportion of infected 'new' host that is sampled is unknown but could be high. For the 'classical' hosts, we selected a representative subset of the patients detected in the area but this sampling is likely to be low. However, the effect of underestimating sampling for the new epidemics would be to underestimate its spread, which is already faster than the classical epidemics. When running the analyses on different phylogenies with half of the 'new' hosts sequences, we find results similar to those obtained with the whole phylogeny, suggesting that our ABC framework is partly robust to sampling biases. In general, implementing a more realistic sampling scheme in the model would be possible but it would require a more detailed model and more data to avoid identifiability issues. Regarding assigning hosts to one of the two types, this was performed by clinicians independently of the sequence data. The main criterion used was the infection stage (acute or chronic), which was complemented by other epidemiological criteria (history of intravenous drug use, blood transfusion, HIV status). Finally, the 'classical' and the 'new' epidemics appear to be spreading on contact networks with different structures. However, such differences are beyond the level of details of the birth-death model we use here and would require a larger dataset for them to be inferred.

To test whether the infection stage (acute vs. chronic) can explain the data better than the existence of two host types, we developed an alternative model where all infected hosts first go through an acute phase before recovering or progressing to the chronic phase. As for the model with two host types, we used three time intervals. Supplementary Figure S9 shows the diagram of the model as well as the corresponding equations. Interestingly, it was almost impossible to simulate phylogenies with this model, most likely because of its intrinsic constrains on assortativity (both acute and chronic infections always generate new acute infections).

To our knowledge, few attempts have been made in phylodynamics to tackle the issue of host population heterogeneity. In 2018, a study used the structured coalescent model to
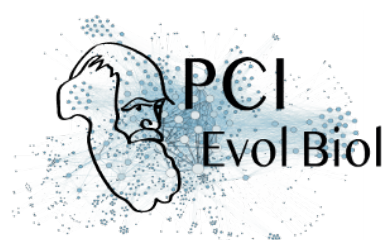
investigate the importance of accounting for so-called 'superspreaders' in the recent Ebola epidemics in West Africa (Volz and Siveroni, 2018). The same year, another study used the birth-death model to study the effect of drug resistance mutations on the R_0 of HIV strains (Kühnert et al., 2018). Both of these are implemented in Beast2. We ran an analysis using the BEAST 2 package bdmm with our data. We were unable to conclude anything from this analysis. However, this is probably due to difficulties in estimating both evolutionary and epidemiological parameters, when in this ABC inference study we inferred epidemiological parameters using a fixed phylogeny.

Overall, we show that our ABC approach, which we validated for simple SIR epidemiological models (Saulnier et al., 2017), can be applied to more elaborate models that current phylo-dynamics methods have difficulties to capture. Further increasing the level of details in the model may require to increase the number of simulations but also to introduce new summary statistics. Another promising perspective would be to combine sequence and incidence data. Although this could not be done here due to the limited sampling, such data integration can readily be done with regression-ABC.
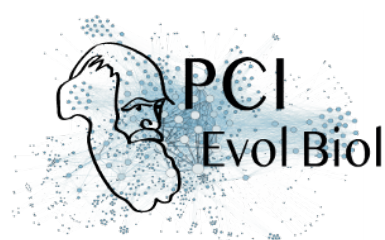
Material and methods

Epidemiological data

The Dat'AIDS cohort is a collaborative network of 23 French HIV treatment centres covering approximately 25% of HIV-infected patients followed in France (Clinicaltrials.gov ref NCT02898987). Host profiles have been established by field epidemiologists based on interviews and risk factors.

HCV sequence data

We included HCV molecular sequences of all MSM patients diagnosed with acute HCV geno-type 1a infection at the Infectious Disease Department of the Hospices Civils de Lyon, France, and for whom NS5B sequencing was performed between January 2014 and December 2017 ($N = 68$). HCV genotype 1a isolated from $N = 145$ non-MSM, HIV-negative, male patients of similar age were analysed by NS5B sequencing at the same time for phylogenetic analysis. This study was conducted following French ethics regulations. All patients gave their written informed consent to allow the use of their personal clinical data. The study was approved by the Ethics Committee of Hospices Civils de Lyon.

HCV testing and sequencing

HCV RNA was detected and quantified using the Abbott RealTime HCV assay (Abbott Molecular, Rungis, France). The NS5B fragment of HCV was amplified between nucleotides 8256

and 8644 by RT-PCR as previously described and sequenced using the Sanger method. Electrophoresis and data collection were performed on a GenomeLab™ GeXP Genetic Analyzer (Beckman Coulter). Consensus sequences were assembled and analysed using the GenomeLab™ sequence analysis software. The genotype of each sample was determined by comparing its sequence with HCV reference sequences obtained from GenBank.

Nucleotide accession numbers

All HCV NS5B sequences isolated in MSM and non-MSM patients reported in this study were submitted to the GenBank database. The list of Genbank accession numbers for all sequences is provided in Appendix.

Dated viral phylogeny

To infer the time-scaled viral phylogeny from the alignment we used a Bayesian Skyline model in BEAST v2.5.2 (Bouckaert et al., 2014). The general time-reversible (GTR) nucleotide substitution model was used with a strict clock rate fixed at $1.3 \cdot 10^{-3}$ based on data from Ref. (Gray et al., 2011) and a gamma distribution with four substitution rate categories. The MCMC was run for 100 million iterations and samples were saved every 100,000 iterations. We selected the maximum clade credibility using TreeAnnotator BEAST2 package. The date of the last common ancestor was estimated to be 1961.95 with a 95% Highest Posterior Density (HPD) of $[1941.846; 1975.516]$. When performing the same inference without the new hosts, we found a similar estimate (1960) and the same 95% HPD of $[1942; 1975]$, which we used as a prior distribution to estimate the origin of the classical hosts t_0 (Table 1).

Epidemiological model and simulations

We assume a Birth-Death model with two hosts types (Supplementary Figure S1) with 'classical' hosts (numbered 1) and new hosts (numbered 2). This model is described by the following system of ordinary differential equations (ODEs):

$$\frac{dI_1}{dt} = a_1 \beta I_1 + (1 - a_2)\nu \beta I_2 - \gamma_1 I_1 \tag{1a}$$

$$\frac{dI_2}{dt} = a_2 \beta \nu I_2 + (1 - a_1)\beta I_1 - \gamma_2 I_2 \tag{1b}$$

In the model, transmission events are possible within each type of hosts and between the two types of hosts at a transmission rate β. Parameter ν corresponds to the transmission rate differential between classical and new hosts. Individuals can be 'removed' at a rate γ_1 from an infectious compartment (I_1 or I_2) via infection clearance, host death or change in host behaviour (e.g. condom use). The assortativity between host types, which can be seen as the percentage of transmissions that occur with hosts from the same type, is captured by parameter a_i.
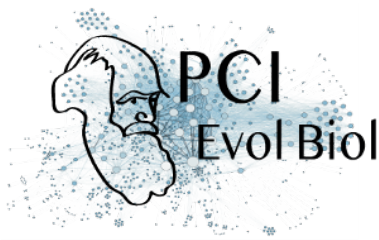
Table 1. Prior distributions for the birth-death model parameters over the three time intervals. t_0 is the date of origin of the epidemics in the studied area, t_1 is the date of introduction of 3$^{\text{rd}}$ generation HCV tests, t_2 is the date of emergence of the epidemic in 'new' hosts and t_3 is the time of the most recent sampled sequence.
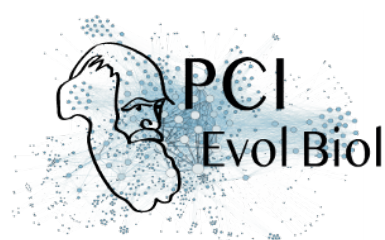
Interval	γ_i	ν	$R^{(1)}$	a_i
$[t_0, t_1]$	$\text{Unif}(0.1, 4)$	0	$\text{Unif}(0.9, 6)$	$\text{Unif}(0.5, 1)$
$[t_1, t_2]$			$\text{Unif}(0.1, 3)$	
$[t_2, t_3]$		$\text{Unif}(0, 1)$ & $\text{Unif}(1, 10)$		

The effective reproduction number (denoted R_t) is the number of secondary cases caused by an infectious individual in a fully susceptible host population (Anderson and May, 1991). We seek to infer the R_t from the classical epidemic, denoted $R^{(1)}$ and defined by $R^{(1)} = \beta/\gamma_1$, as well as the R_t of the new epidemic, denoted $R^{(2)}$ and defined by $R^{(2)} = \nu\beta/\gamma_2 = \nu R^{(1)}\gamma_1/\gamma_2$.

The doubling time of an epidemic (t_D) corresponds to the time required for the number of infected hosts to double in size. It is usually estimated in the early stage of an epidemic when epidemic growth can assumed to be exponential. To calculate it, we assume perfect assortativity ($a_1 = a_2 = 1$) and approximate the initial exponential growth rate by $\beta - \gamma_1$ for 'classical' hosts and $\nu\beta - \gamma_2$ for 'new' hosts. Following (Wallinga and Lipsitch, 2007), we obtain $t_D^{(1)} = \ln(2)/(\beta - \gamma_1)$ and $t_D^{(2)} = \ln(2)/(\nu\beta - \gamma_2)$.

We consider three time intervals. During the first interval $[t_0, t_1]$, t_0 being the year of the origin of the epidemic in the area of Lyon, we assume that only classical hosts are present. The second interval $[t_1, t_2]$, begins in $t_1 = 1997.3$ with the introduction of the third generation HCV tests, which we assume to have affected $R^{(1)}$ through the decrease of the transmission rate β. Finally, the 'new' hosts appear during the last interval $[t_2, t_3]$, where t_2, which we infer, is the date of origin of the second outbreak. The final time (t_3) is set by the most recent sampling date in our dataset (2018.39). The prior distributions used are summarized in Table 1 and shown in Figure 2. Given the phylogeny structure suggesting a high degree of assortativity, we assume the assortativity parameters, a_1 and a_2, to be higher than 50%. For the prior distribution of parameter ν, we combined a uniform distribution from 0 to 1 with a uniform distribution from 1 to 10. This was done to ensure that the probability to have $\nu < 1$ is equal to the probability to have $\nu > 1$.

To simulate phylogenies, we use our TiPS simulator (Danesh, Saulnier, et al., 2020) implemented in R via the Rcpp package. This is done in a two-step procedure. First, epidemiological trajectories are simulated using the compartmental model in equation 1 and Gillespie's stochastic event-driven simulation algorithm (Gillespie, 1976). The number of individuals in each compartment and the reactions occurring through the simulations of trajectories, such as recovery or transmission events, are recorded. Using the target phylogeny, we know when

sampling events occur. For each simulation, each sampling date is randomly associated to a host compartment using the observed fraction of each infection type (here 68% of the dates associated with 'classical' hosts type and 32% with 'new' hosts). Once the sampling dates are added to the trajectories, we move to the second step, which involves simulating the phylogeny. This step starts from the last sampling date and follows the epidemiological trajectory through a coalescent process, that is backwards-in-time. Each backward step in the trajectory can induce a tree modification given a probability and the population size: a sampling event leads to a labelled leaf in the phylogeny, a transmission event can lead to the coalescence of two sampled lineages or to no modification of the phylogeny (if one of the lineages is not sampled).

We implicitly assume that the sampling rate is low, which is consistent with the limited number of sequences in the dataset. We also assume that the virus can still be transmitted after sampling.

We simulate $60,000$ phylogenies from known parameter sets drawn in the prior distributions shown in Table 1. These are used to perform the rejection step and build the regression model in the Approximate Bayesian Computation (ABC) inference.

ABC inference

Summary statistics

Phylogenies are rich objects and to compare them we break them into summary statistics. These are chosen to capture the epidemiological information of interest. In particular, following an earlier study, we use summary statistics from branch lengths, tree topology, and lineage-through-time (LTT) (Saulnier et al., 2017), and summary statistics based on the Laplacian spectrum using the spectR function of the RPANDA R package (Lewitus and Morlon, 2016).

We also compute new summary statistics to extract information regarding the heterogeneity of the population, the assortativity, and the difference between the two R. To do so, we annotate each internal node by associating it with a probability to be in a particular state (here the host type, 'classical' or 'new'). We assume that this probability is given by the ratio

$$P(Y) = \frac{\text{number of descendent leaves labelled } Y}{\text{number of descendent leaves}} \qquad (2)$$

where Y is a state (or host type). Each node is therefore annotated with n ratios, n being the number of possible states. Since in our case $n = 2$, we only follow one of the labels and use the mean and the variance of the distribution of the ratios (one for each node) as summary statistics.

In a phylogeny, cherries are pairs of leaves that are adjacent to a common ancestor. There are $n(n + 1)/2$ categories of cherries. Here, we compute the proportion of homogeneous cherries for each label and the proportion of heterogeneous cherries. We also consider pitchforks, which we define as a cherry and a leaf adjacent to a common ancestor, and introduce
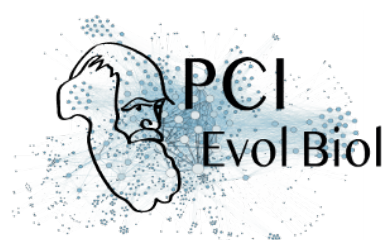
three categories: homogeneous pitchforks, pitchforks whose cherries are homogeneous for a label and whose leaf is labelled with another trait, and pitchforks whose cherries are heterogeneous.

The Lineage-Through-Time (LTT) plot displays the number of lineages of a phylogeny over time. In this plot, the number of lineages is incremented by one every time there is a new branch in the phylogeny and is decreased by one every time there is a new leaf in the phylogeny. We use the ratios defined for each internal node to build an LTT plot for each label type, which we refer to as 'LTT label plot'. After each branching event in phylogeny, we increment the number of lineages by the value of the ratio of the internal node for the given label. This number of lineages is decreased by one every time there is a leaf in the phylogeny. In the end, we obtain $n = 2$ LTT label plots.

Finally, for each label, we compute some of our branch lengths summary statistics on homogeneous clades and heterogeneous clades present in the phylogeny. Homogeneous clades are defined by their root having a ratio of 1 for one type of label and their size being greater than $N_{\min}$. For heterogeneous clades, we keep the size criterion and impose that the ratio is smaller than 1 but greater than a threshold ϵ. After preliminary analyses, we set $N_{\min} = 4$ leaves and $\epsilon = 0.7$. We then obtain a set of homogeneous clades and a set of heterogeneous clades, the branch lengths of which we pool into two sets to compute the summary statistics of heterogeneous and homogeneous clades. Note that we always select the largest clade, for both homogeneous and heterogeneous cases, to avoid redundancy.

Regression-ABC

We first measure multicollinearity between summary statistics using variance inflation factors (VIF). Each summary statistic is kept if its VIF value is lower than 10. This stepwise VIF test leads to the selection of 101 summary statistics out of 330.

We then use the abc function from the abc R package (Csillery et al., 2012) to infer posterior distributions generated using only the rejection step. Finally, we perform linear adjustment using an elastic net regression.

The abc function performs a classical one-step rejection algorithm (Beaumont et al., 2002) using a tolerance parameter P_{δ}, which represents a percentile of the simulations that are close to the target. To compute the distance between a simulation and the target, we use the Euclidian distance between normalized simulated vectors of summary statistics and the normalized target vector.

Before linear adjustment, the abc function performs smooth weighting using an Epanechnikov kernel (Beaumont et al., 2002). Then, using the glmnet package in R, we implement an elastic-net (EN) adjustment, which balances the Ridge and the LASSO regression penalties (Zou and Hastie, 2005). Since the EN performs a linear regression, it is not subject to the risk of over-fitting that may occur for non-linear regressions (e.g. when using neural networks, support vector machines or random forests).

In the end, we obtain posterior distributions for t_0, t_2, a_1, a_2, ν, γ_1, γ_2, $R^{(1),t_1}$ and $R^{(1),t_2}$ using our ABC-EN regression model with $P_\delta = 0.05$.

Parametric bootstrap and cross-validation

Our goodness-of-fit validation consists in simulating $10,000$ additional phylogenies from parameter sets drawn in posterior distributions. We then compute summary statistics and perform a goodness of fit using the gfitpca function from the abc R package (Csillery et al., 2012). The function performs principal component analysis (PCA) using the simulated summary statistics. It displays envelopes containing a given percentage, here 90%, of the simulations. The projection of the observed summary statistics is displayed to check if they are contained or not in the envelopes. If the posterior distribution is informative, we expect the target data to be contained in the envelope. This analysis was performed either on the posterior distribution, or on a uniform distribution based on the 95% HPD posterior distribution of each parameter, the latter being less informative.

To assess the robustness of our ABC-EN method to infer epidemiological parameters of our BD model, we also perform a 'leave-one-out' cross-validation as in (Saulnier et al., 2017). This consists in inferring posterior distributions of the parameters from one simulated phylogeny, assumed to be the target phylogeny, using the ABC-EN method with the remaining $59,999$ simulated phylogenies. We run the cross-validation 100 times with 100 different target phylogenies. We consider three parameter distributions θ: the prior distribution, the prior distribution reduced by the feasibility of the simulations and the ABC inferred posterior distribution. For each of these parameter distributions, we measure the median and compute, for each simulation scenario, the mean relative error (MRE) such as:

$$MRE = \frac{1}{100} \sum_{i=1}^{100} \left| \frac{\theta_i}{\Theta} - 1 \right| \tag{3}$$

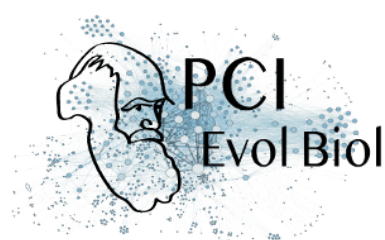where Θ is the true value.

Data accessibility

Data are available online: link or DOI of the webpage hosting the data

Supplementary material

Script and codes are available online: link or DOI of the webpage hosting the script and codes

Acknowledgements

We thank Jūlija Pečerska for her help with Beast2.
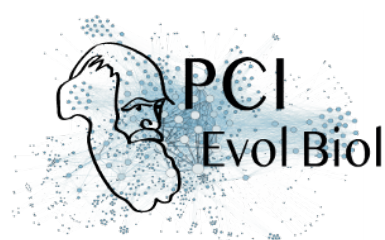
Conflict of interest disclosure

The authors of this preprint declare that they have no financial conflict of interest with the content of this article. SA is a recommender for PCI Evol Biol.

References

AASLD/IDSA HCV Guidance Panel (Sept. 2015). Hepatitis C guidance: AASLD-IDSA recommendations for testing, managing, and treating adults infected with hepatitis C virus. *Hepatology* 62, 932–954. doi: 10.1002/hep.27950.

Alter MJ (2006). Epidemiology of viral hepatitis and HIV co-infection. *J. Hepatol.* 44, S6–9. doi: 10.1016/j.jhep.2005.11.004.

Anderson RM and RM May (1991). *Infectious Diseases of Humans. Dynamics and Control*. Oxford: Oxford University Press.

Beaumont MA, W Zhang, and DJ Balding (2002). Approximate Bayesian Computation in Population Genetics. *Genetics* 162, 2025–2035.

Béguelin C, A Suter, E Bernasconi, J Fehr, H Kovari, HC Bucher, M Stoeckle, M Cavassini, M Rougemont, P Schmid, G Wandeler, and A Rauch (2018). Trends in HCV treatment uptake, efficacy and impact on liver fibrosis in the Swiss HIV Cohort Study. en. *Liver International* 38, 424–431. issn: 1478-3231. doi: 10.1111/liv.13528.

Berenguer J, I Jarrín, L Pérez-Latorre, V Hontañón, MJ Vivancos, J Navarro, MJ Téllez, JM Guardiola, JA Iribarren, A Rivero-Juárez, M Márquez, A Artero, L Morano, I Santos, J Moreno, MC Fariñas, MJ Galindo, MA Hernando, M Montero, C Cifuentes, P Domingo, J Sanz, L Domínguez, OL Ferrero, B De la Fuente, C Rodríguez, S Reus, J Hernández-Quero, G Gaspar, L Pérez-Martínez, C García, L Force, S Veloso, JE Losa, J Vilaró, E Bernal, S Arponen, AJ Ortí, Á Chocarro, R Teira, G Alonso, R Silvariño, A Vegas, P Geijo, J Bisbe, H Esteban, and J González-García (Jan. 2018). Human Immunodeficiency Virus/Hepatits C Virus Coinfection in Spain: Elimination Is Feasible, but the Burden of Residual Cirrhosis Will Be Significant. *Open Forum Infect. Dis.* 5. doi: 10.1093/ofid/ofx258.
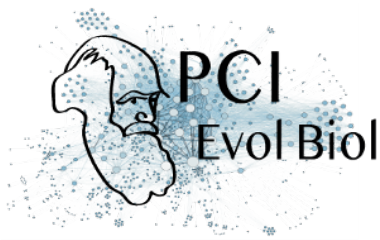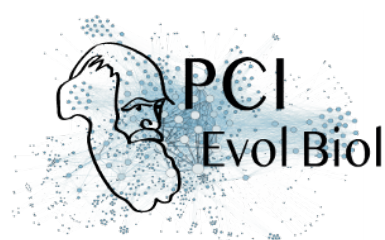
Boerekamps A, GE van den Berk, FN Lauw, EM Leyten, ME van Kasteren, A van Eeden, D Posthouwer, MA Claassen, AS Dofferhoff, DWM Verhagen, WF Bierman, KD Lettinga, FP Kroon, CE Delsing, PH Groeneveld, R Soetekouw, EJ Peters, SJ Hullegie, S Popping, DAMC van de Vijver, CA Boucher, JE Arends, and BJ Rijnders (Apr. 2018). Declining Hepatitis C Virus (HCV) Incidence in Dutch Human Immunodeficiency Virus-Positive Men Who Have Sex With Men After Unrestricted Access to HCV Therapy. en. *Clin. Infect. Dis.* 66, 1360–1365. doi: 10.1093/cid/cix1007.

Bouckaert R, J Heled, D Kühnert, T Vaughan, CH Wu, D Xie, MA Suchard, A Rambaut, and AJ Drummond (2014). BEAST 2: A Software Platform for Bayesian Evolutionary Analysis. *PLoS Comput. Biol.* 10, e1003537. doi: 10.1371/journal.pcbi.1003537.

Breban R, N Arafa, S Leroy, A Mostafa, I Bakr, L Tondeur, M Abdel-Hamid, W Doss, G Esmat, MK Mohamed, and A Fontanet (2014). Effect of preventive and curative interventions on hepatitis C virus transmission in Egypt (ANRS 1211): a modelling study. *Lancet Glob. Health* 2, e541–e549. doi: 10.1016/S2214-109X(14)70188-3.

Csillery K, O Francois, and MGB Blum (2012). abc: an R package for approximate Bayesian computation (ABC). *Methods Ecol. Evol.* doi: http://dx.doi.org/10.1111/j.2041-210X.2011.00179.x.

D'Oliveira JA, N Voirin, R Allard, D Peyramond, C Chidiac, JL Touraine, J Fabry, C Trepo, and P Vanhems (2005). Prevalence and sexual risk of hepatitis C virus infection when human immunodeficiency virus was acquired through sexual intercourse among patients of the Lyon University Hospitals, France, 1992-2002. *J. Viral. Hepat.* 12, 330–332. doi: 10.1111/j.1365-2893.2005.00583.x.

Danesh G, E Saulnier, O Gascuel, M Choisy, and S Alizon (2020). Simulating trajectories and phylogenies from population dynamics models with TiPS. *bioRxiv*, 2020.11.09.373795. doi: 10.1101/2020.11.09.373795.

Danesh G, V Virlogueux, C Ramière, C Charre, L Cotte, and S Alizon (2020). Quantifying transmission dynamics of acute hepatitis C virus infections in a heterogeneous population using sequence data. *bioRxiv* 689158, ver. 5 peer-reviewed and recommended by *PCI Evol Biol*. doi: https://doi.org/10.1101/689158.

European Union HCV Collaborators (2017). Hepatitis C virus prevalence and level of intervention required to achieve the WHO targets for elimination in the European Union by 2030: a modelling study. eng. *Lancet Gastroenterol. Hepatol.* 2, 325–336. issn: 2468-1253. doi: 10.1016/S2468-1253(17)30045-6.

Frost SD, OG Pybus, JR Gog, C Viboud, S Bonhoeffer, and T Bedford (2015). Eight challenges in phylodynamic inference. *Epidemics* 10, 88–92.

Gillespie DT (1976). A general method for numerically simulating the stochastic time evolution of coupled chemical reactions. *J. Comput. Physics* 22, 403–434. doi: 10.1016/0021-9991(76)90041-3.

Gray RR, J Parker, P Lemey, M Salemi, A Katzourakis, and OG Pybus (2011). The mode and tempo of hepatitis C virus evolution within and among hosts. *BMC Evol. Biol.* 11, 131. doi: 10.1186/1471-2148-11-131.

Grenfell BT, OG Pybus, JR Gog, JL Wood, JM Daly, JA Mumford, and EC Holmes (2004). Unifying the epidemiological and evolutionary dynamics of pathogens. *Science* 303, 327–32. doi: 10.1126/science.1090727.

Heffernan A, GS Cooke, S Nayagam, M Thursz, and TB Hallett (2019). Scaling up prevention and treatment towards the elimination of hepatitis C: a global mathematical model. *Lancet* 393, 1319–1329. doi: 10.1016/S0140-6736(18)32277-3.

Joy JB, RM McCloskey, T Nguyen, RH Liang, Y Khudyakov, A Olmstead, M Krajden, JW Ward, PR Harrigan, JSG Montaner, and AFY Poon (2016). The spread of hepatitis C virus genotype 1a in North America: a retrospective phylogenetic study. *Lancet Infect. Dis.* 16, 698–702. doi: 10.1016/S1473-3099(16)00124-9.

Klein MB et al. (2016). Risk of End-Stage Liver Disease in HIV-Viral Hepatitis Coinfected Persons in North America From the Early to Modern Antiretroviral Therapy Eras. *Clin. Infect. Dis.* 63, 1160–1167. doi: 10.1093/cid/ciw531.

Kovari H, B Ledergerber, M Cavassini, J Ambrosioni, A Bregenzer, M Stöckle, E Bernasconi, R Kouyos, R Weber, and A Rauch (Sept. 2015). High hepatic and extrahepatic mortality and low treatment uptake in HCV-coinfected persons in the Swiss HIV cohort study between 2001 and 2013. *J. Hepatol.* 63, 573–580. issn: 0168-8278. doi: 10.1016/j.jhep.2015.04.019.

Kühnert D, R Kouyos, G Shirreff, J Pečerska, AU Scherrer, J Böni, S Yerly, T Klimkait, V Aubert, HF Günthard, T Stadler, S Bonhoeffer, and the Swiss HIV Cohort Study (2018). Quantifying the fitness cost of HIV-1 drug resistance mutations through phylodynamics. *PLoS Pathog.* 14, e1006895. doi: 10.1371/journal.ppat.1006895.

Kwon JA, J Iversen, L Maher, MG Law, and DP Wilson (2009). The Impact of Needle and Syringe Programs on HIV and HCV Transmissions in Injecting Drug Users in Australia: A Model-Based Analysis. *JAIDS Journal of Acquired Immune Deficiency Syndromes* 51, 462. doi: 10.1097/QAI.0b013e3181a2539a.

Laar T van de, O Pybus, S Bruisten, D Brown, M Nelson, S Bhagani, M Vogel, A Baumgarten, ML Chaix, M Fisher, H Gőtz, GV Matthews, S Neifer, P White, W Rawlinson, S Pol, J Rockstroh, R Coutinho, GJ Dore, GM Dusheiko, and M Danta (2009). Evidence of a Large, International Network of HCV Transmission in HIV-Positive Men Who Have Sex With Men. *Gastroenterology* 136, 1609–1617. issn: 0016-5085. doi: 10.1053/j.gastro.2009.02.006.

Laar TJW van de, AK van der Bij, M Prins, SM Bruisten, K Brinkman, TA Ruys, JTM van der Meer, HJC de Vries, JW Mulder, M van Agtmael, S Jurriaans, KC Wolthers, and RA Coutinho (July 2007). Increase in HCV Incidence among Men Who Have Sex with Men in Amsterdam Most Likely Caused by Sexual Transmission. *J Infect. Dis.* 196, 230–238. doi: 10.1086/518796.

Lewitus E and H Morlon (2016). Characterizing and comparing phylogenies from their laplacian spectrum. *Syst. Biol.* 65, 495–507. issn: 1076836X. doi: 10.1093/sysbio/syv116.
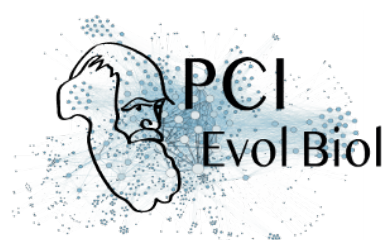
Magiorkinis G, E Magiorkinis, D Paraskevis, SYW Ho, B Shapiro, OG Pybus, JP Allain, and A Hatzakis (2009). The Global Spread of Hepatitis C Virus 1a and 1b: A Phylodynamic and Phylogeographic Analysis. en. *PLOS Med.* 6, e1000198. doi: 10.1371/journal.pmed.1000198.

Messina JP, I Humphreys, A Flaxman, A Brown, GS Cooke, OG Pybus, and E Barnes (2015). Global distribution and prevalence of hepatitis C virus genotypes. en. *Hepatology* 61, 77–87. doi: 10.1002/hep.27259.

Pitcher AB, A Borquez, B Skaathun, and NK Martin (2018). Mathematical modeling of hepatitis c virus (HCV) prevention among people who inject drugs: A review of the literature and insights for elimination strategies. *J. theor. Biol.* doi: 10.1016/j.jtbi.2018.11.013.

Pradat P, E Caillat-Vallet, F Sahajian, F Bailly, G Excler, M Sepetjan, C Trépo, and J Fabry (2001). Prevalence of hepatitis C infection among general practice patients in the Lyon area, France. *Eur. J. Epidemiol.* 17, 47–51. doi: 10.1023/A:1010902614443.

Pradat P, T Huleux, F Raffi, P Delobel, MA Valantin, I Poizot-Martin, P Pugliese, J Reynes, D Rey, B Hoen, A Cabie, F Bani-Sadr, A Cheret, C Duvivier, C Jacomet, A Fresard, L Hustache-Mathieu, L Cotte, and tDs Group (May 2018). Incidence of new hepatitis C virus infection is still increasing in French MSM living with HIV. *AIDS* 32, 1077. issn: 0269-9370. doi: 10.1097/QAD.0000000000001789.

Pradat P, P Pugliese, et al. (Sept. 2017). Direct-acting antiviral treatment against hepatitis C virus infection in HIV-Infected patients – "En route for eradication"? *J. Infection* 75, 234–241. doi: 10.1016/j.jinf.2017.05.008.

Pybus OG, MA Charleston, S Gupta, A Rambaut, EC Holmes, and PH Harvey (2001). The epidemic behavior of the hepatitis C virus. *Science* 292, 2323–5. doi: 10.1126/science.1058321.

Pybus OG, A Cochrane, EC Holmes, and P Simmonds (2005). The hepatitis C virus epidemic among injecting drug users. *Inf. Gen. Evol.* 5, 131–139. issn: 1567-1348. doi: 10.1016/j.meegid.2004.08.001.

Ramière C, C Charre, P Miailhes, F Bailly, S Radenne, AC Uhres, C Brochier, M Godinot, P Chiarello, P Pradat, L Cotte, M Astrie, C Augustin-Normand, B François, F Biron, A Boibieux, C Brochier, E Braun, F Brunel, C Charre, P Chiarello, C Chidiac, L Cotte, T Ferry, M Godinot, O Guillaud, J Koffi, JM Livrozet, D Makhloufi, P Miailhes, T Perpoint, P Pradat, S Radenne, C Ramière, I Schlienger, C Scholtes, I Schuffenecker, JC Tardy, MA Trabaud, and AC Uhres (2019). Patterns of Hepatitis C Virus Transmission in Human Immunodeficiency Virus (HIV)–infected and HIV-negative Men Who Have Sex With Men. *Clin. Infect. Dis.* 69, 2127–2135. doi: 10.1093/cid/ciz160.

Romero-Severson EO, I Bulla, and T Leitner (2016). Phylogenetically resolving epidemiologic linkage. *Proc. Nat. Acad. Sci. USA* 113, 2690–2695. doi: 10.1073/pnas.1522930113.

Rosenthal E, D Salmon-Céron, C Lewden, V Bouteloup, G Pialoux, F Bonnet, M Karmochkine, T May, M François, C Burty, E Jougla, D Costagliola, P Morlat, G Chêne, and P Cacoub (2009). Liver-related deaths in HIV-infected patients between 1995 and 2005 in the French GERMIVIC Joint Study Group Network (Mortavic 2005 Study in collaboration with the Mortalité
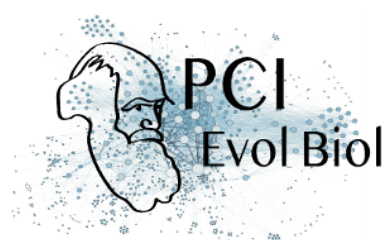
2005 survey, ANRS EN19). en. *HIV Medicine* 10, 282–289. doi: 10.1111/j.1468-1293.2008. 00686.x.

Sahajian F, F Bailly, P Vanhems, B Fantino, C Vannier-Nitenberg, J Fabry, and C Trepo (2011). A randomized trial of viral hepatitis prevention among underprivileged people in the Lyon area of France. en. *J Public Health* 33, 182–192. doi: 10.1093/pubmed/fdq071.

Salazar-Vizcaya L, RD Kouyos, C Zahnd, G Wandeler, M Battegay, KEA Darling, E Bernasconi, A Calmy, P Vernazza, H Furrer, M Egger, O Keiser, and A Rauch (2016). Hepatitis C virus transmission among human immunodeficiency virus-infected men who have sex with men: Modeling the effect of behavioral and treatment interventions. *Hepatology* 64, 1856–1869. doi: 10.1002/hep.28769.

Saulnier E, O Gascuel, and S Alizon (2017). Inferring epidemiological parameters from phylogenies using regression-ABC: A comparative study. *PLOS Comput. Biol.* 13, e1005416. doi: 10.1371/journal.pcbi.1005416.

Stadler T, D Kühnert, S Bonhoeffer, and AJ Drummond (2013). Birth-death skyline plot reveals temporal changes of epidemic spread in HIV and hepatitis C virus (HCV). *Proc. Natl. Acad. Sci. USA* 110, 228–33. doi: 10.1073/pnas.1207965110.

Sweeting MJ, D De Angelis, M Hickman, and AE Ades (2008). Estimating hepatitis C prevalence in England and Wales by synthesizing evidence from multiple data sources. Assessing data conflict and model fit. *Biostatistics* 9, 715–734. issn: 1465-4644. doi: 10.1093/biostatistics/kxn004.

Virlogeux V, F Zoulim, P Pugliese, I Poizot-Martin, MA Valantin, L Cuzin, J Reynes, E Billaud, T Huleux, F Bani-Sadr, D Rey, A Frésard, C Jacomet, C Duvivier, A Cheret, L Hustache-Mathieu, B Hoen, A Cabié, L Cotte, and the Dat'AIDS Study Group (Dec. 2017). Modeling HIV-HCV coinfection epidemiology in the direct-acting antiviral era: the road to elimination. *BMC Medicine* 15, 217. doi: 10.1186/s12916-017-0979-1.

Volz EM, K Koelle, and T Bedford (2013). Viral phylodynamics. *PLoS Comput. Biol.* 9, e1002947. doi: 10.1371/journal.pcbi.1002947.

Volz EM and I Siveroni (2018). Bayesian phylodynamic inference with complex models. en. *PLoS Comput. Biol.* 14, e1006546. doi: 10.1371/journal.pcbi.1006546.

Wallinga J and M Lipsitch (2007). How generation intervals shape the relationship between growth rates and reproductive numbers. *Proc. R. Soc. Lond. B* 274, 599–604. doi: 10.1098/rspb.2006.3754.

Wandeler G, T Gsponer, A Bregenzer, HF Günthard, O Clerc, A Calmy, M Stöckle, E Bernasconi, H Furrer, and A Rauch (2012). Hepatitis C Virus Infections in the Swiss HIV Cohort Study: A Rapidly Evolving Epidemic. *Clin. Infect. Dis.* 55, 1408–1416. doi: 10.1093/cid/cis694.

Worby CJ, M Lipsitch, and WP Hanage (2017). Shared Genomic Variants: Identification of Transmission Routes Using Pathogen Deep-Sequence Data. *Am. J. Epidemiol.* 186, 1209–1216. issn: 0002-9262. doi: 10.1093/aje/kwx182.

Wymant C, M Hall, O Ratmann, D Bonsall, T Golubchik, M de Cesare, A Gall, M Cornelissen, C Fraser, and STOP-HCV Consortium, The Maela Pneumococcal Collaboration, and The
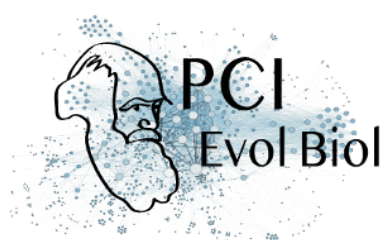
BEEHIVE Collaboration (2018). PHYLOSCANNER: Inferring Transmission from Within- and Between-Host Pathogen Genetic Diversity. *Mol. Biol. Evol.* 35, 719–733. doi: 10.1093/molbev/msx304.

Zou H and T Hastie (2005). Regularization and Variable Selection via the Elastic Net. *J. R. Stat. Soc. B* 67, 301–320. issn: 1369-7412.
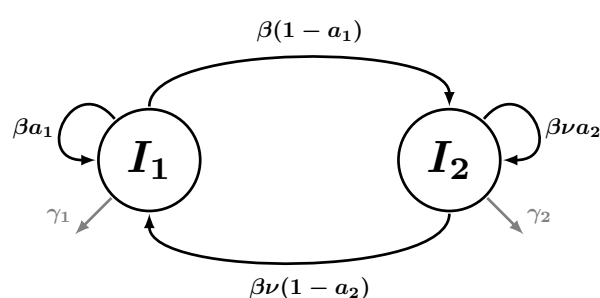
Appendix

$$\beta(1 - a_1)$$

$$\beta a_1 \quad I_1 \qquad I_2 \quad \beta \nu a_2$$

$$\gamma_1 \qquad \qquad \gamma_2$$

$$\beta \nu (1 - a_2)$$

Figure S1. Diagram of the birth-death model with host heterogeneity. The intensity of the colour is proportional to the correlation coefficients.
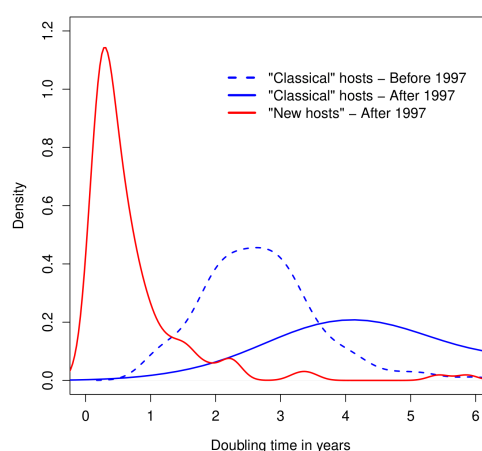
Figure S2. Densities of the inferred doubling times. The density of the doubling time for the 'classical' hosts before 1997 is in blue dashed line, and after 1997 in blue solid line. The density of the doubling time for the 'new' hosts is in red. ($t_D^{(2),t3}$).
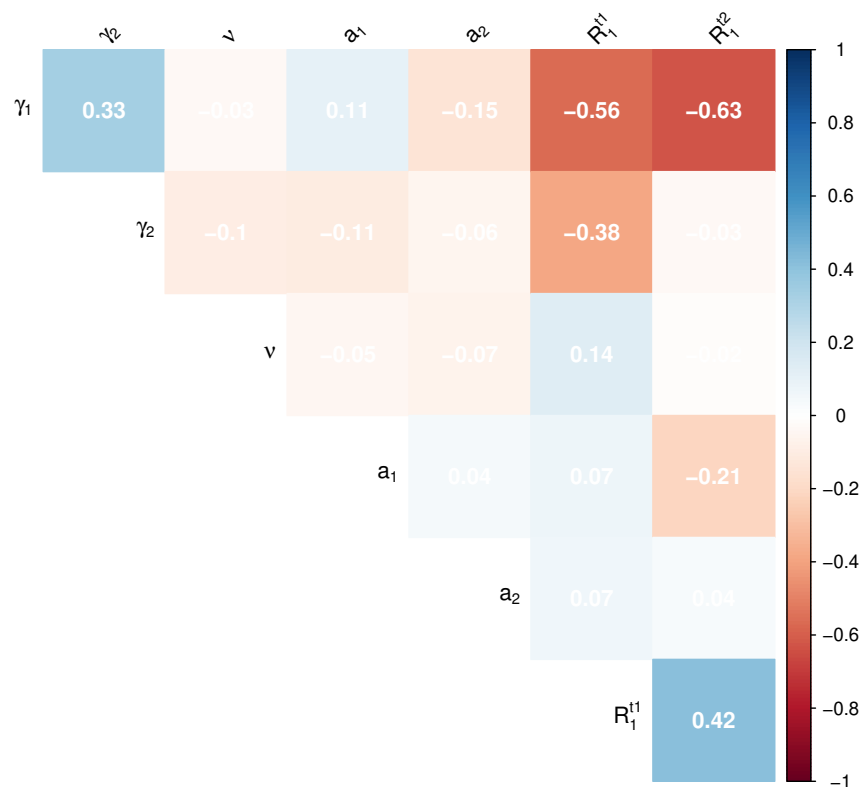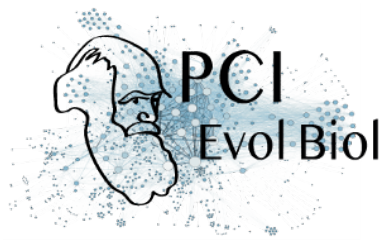
Figure S3. Correlation heat map between the posterior distributions for the model parameters. The intensity of the colour is proportional to the correlation coefficients.
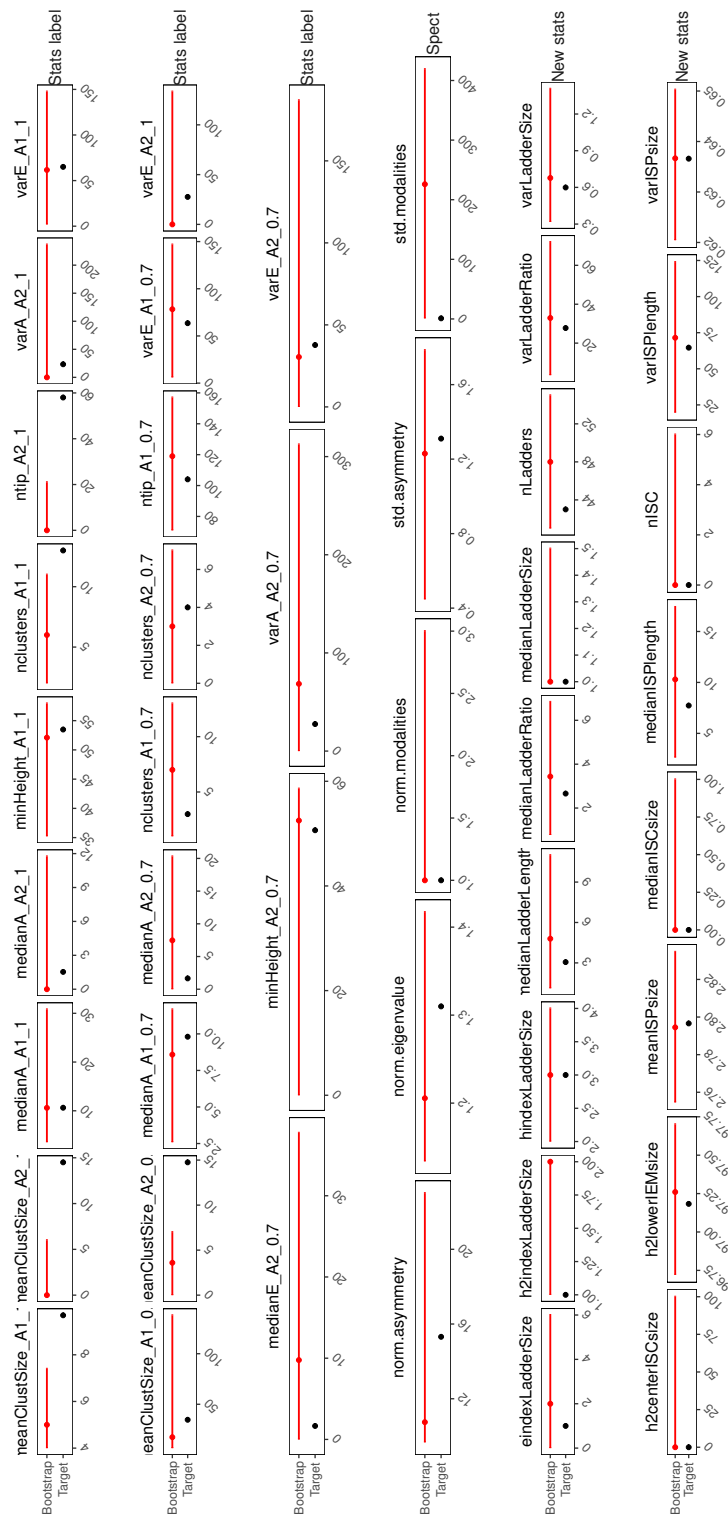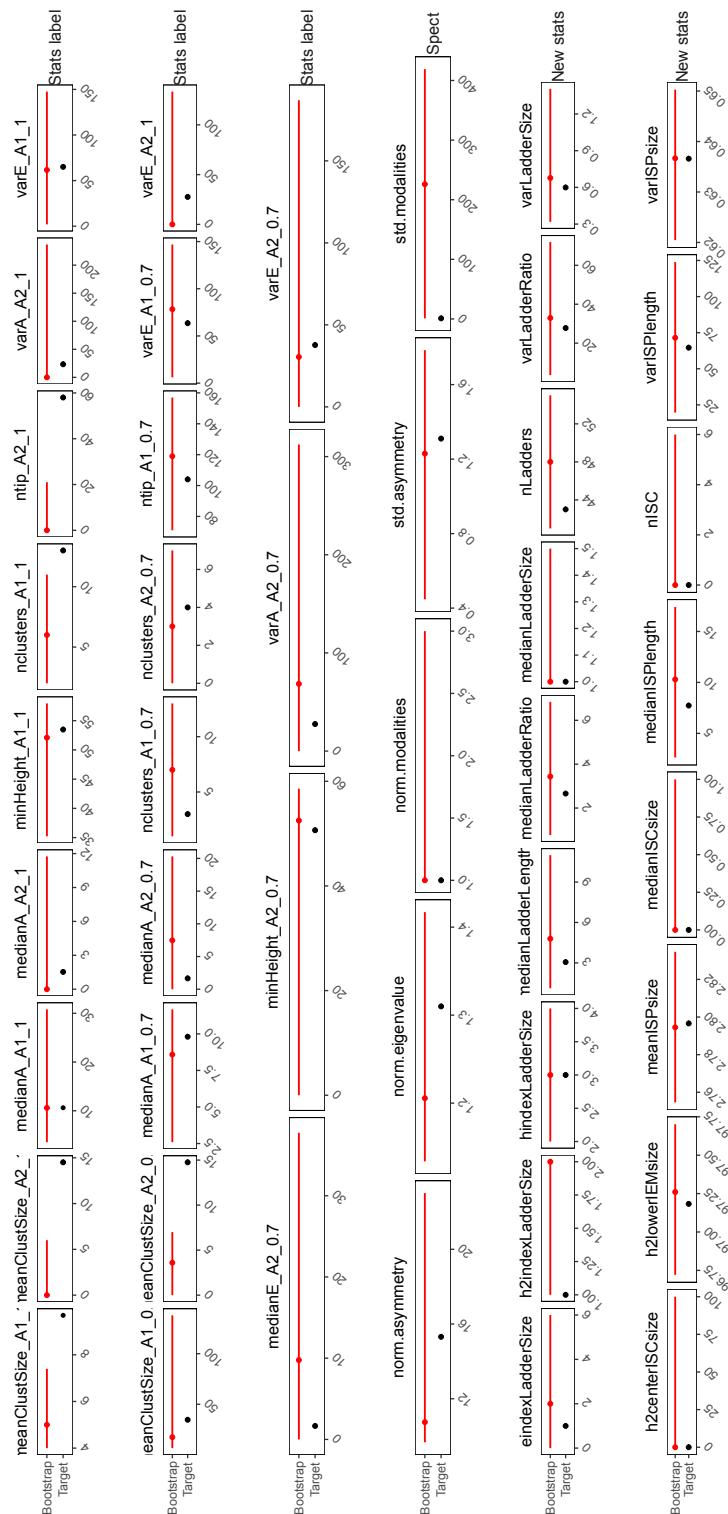
Figure S4. Distributions of selected summary statistics. The dots represent the median and the horizontal lines represent the 95% HPD. Red distributions correspond to the summary statistics computed from the 10,000 phylogenies simulated from the posterior distribution. Black dots represent the values of selected summary statistics computed from the target phylogeny. Summary statistics are represented by group.

Figure S4. Distributions of selected summary statistics. The dots represent the median and the horizontal lines represent the 95% HPD. Red distributions correspond to the summary statistics computed from the 10,000 phylogenies simulated from the posterior distribution. Black dots represent the values of selected summary statistics computed from the target phylogeny. Summary statistics are represented by group.
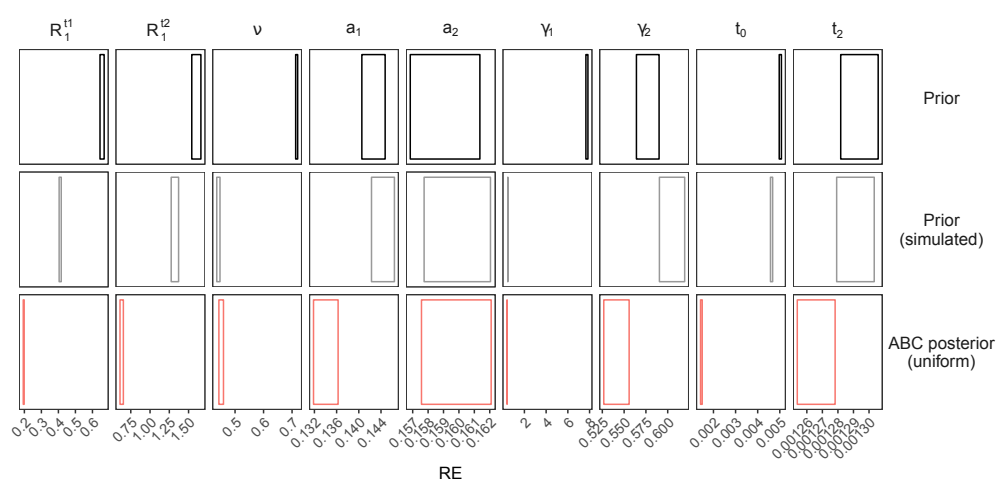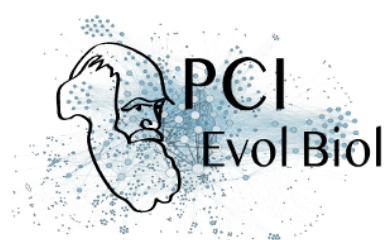
Figure S5. Cross-validation results. Each column corresponds to one of the inferred parameters. The first line shows the prior distribution. The second line shows the distribution of values for which a phylogeny could be simulated. The third line shows the inference after then ABC. For the rejection step of the ABC, the tolerance level was set to $P_\delta = 0.05$. The rectangles show the mean relative errors and their standard errors computed for 100 target sets with known values (see the Methods).
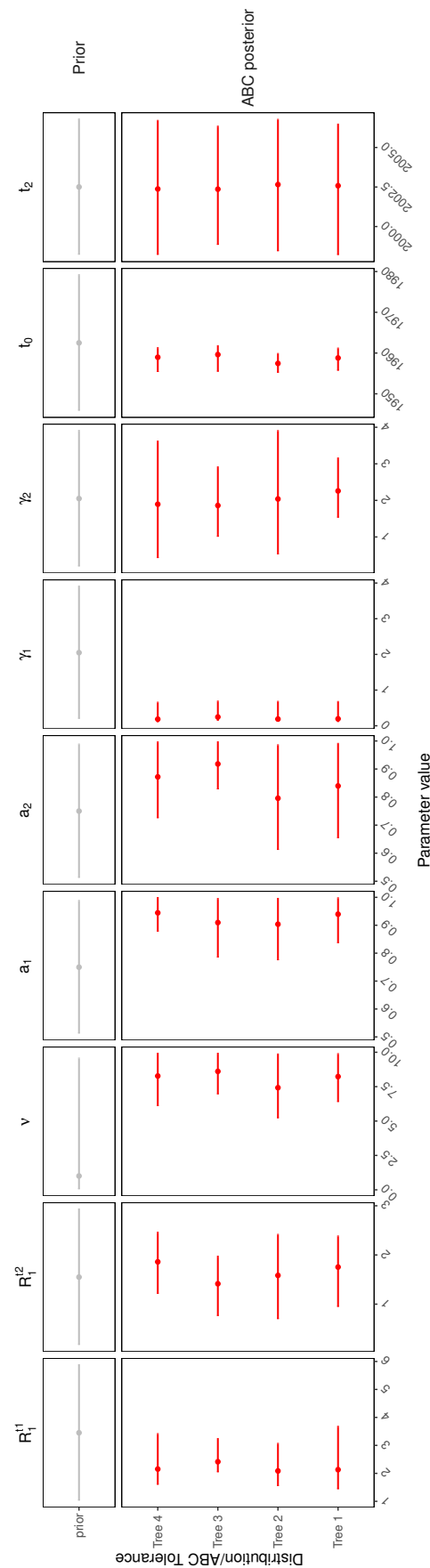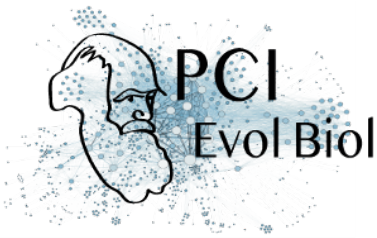
Figure S6. Posterior distributions estimated from different phylogenies inferred using half of the 'new' hosts' sequences. The first line represents the prior (in grey), the last line the full target tree (in red), and all the intermediate lines phylogenies where half of the 'new' host sequences were removed at random.
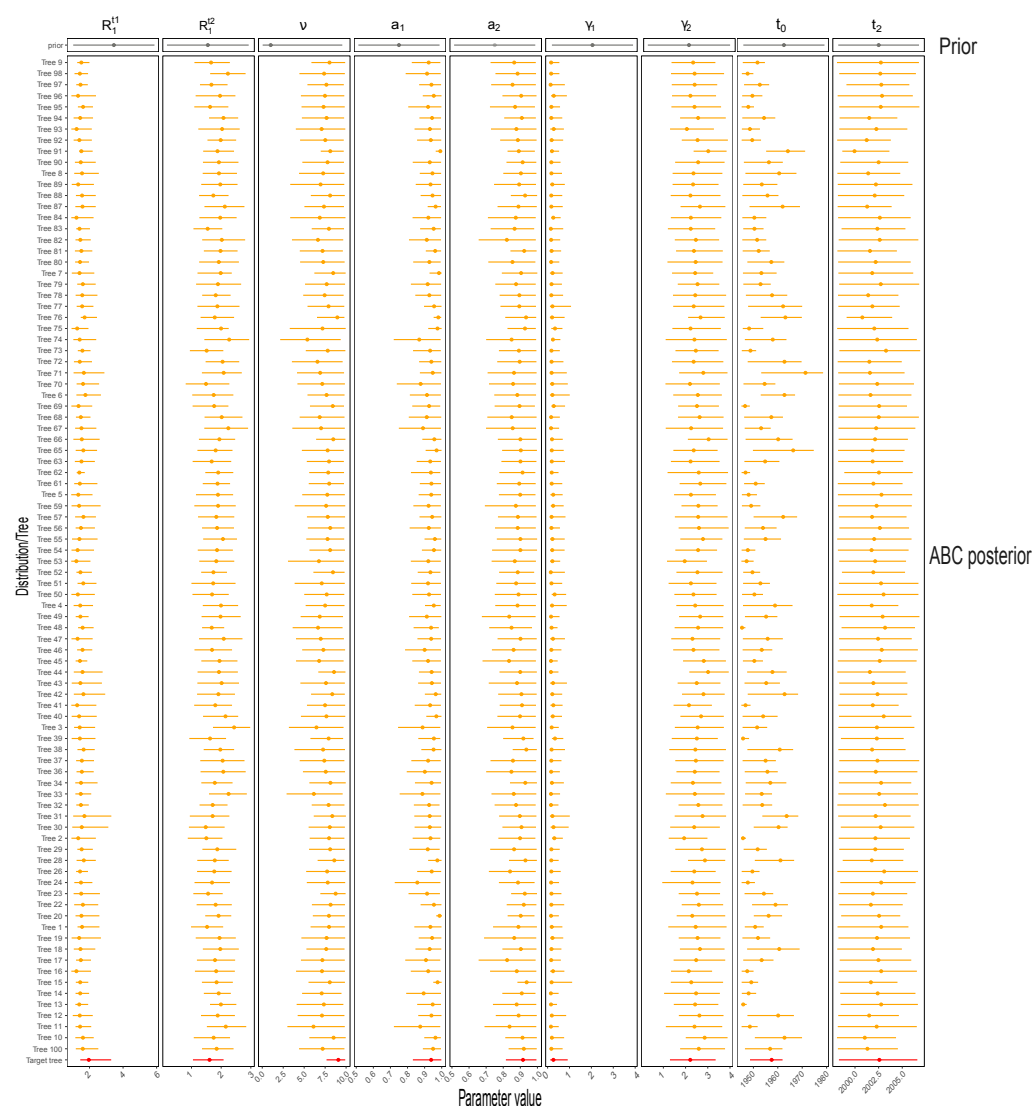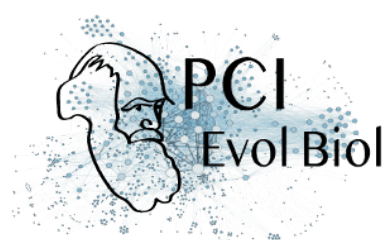
Figure S7. Variation in posterior distribution estimated from different inferred phylogenies. The dots represent the median and the horizontal lines represent the 95% highest posterior density (HPD) of each distribution. Grey distributions correspond to the prior, orange distributions correspond to the different posterior distributions computed from 100 phylogenies drawn at random in the posterior distribution of trees inferred by Beast2 and red distributions correspond to the ABC-EN posterior distributions.
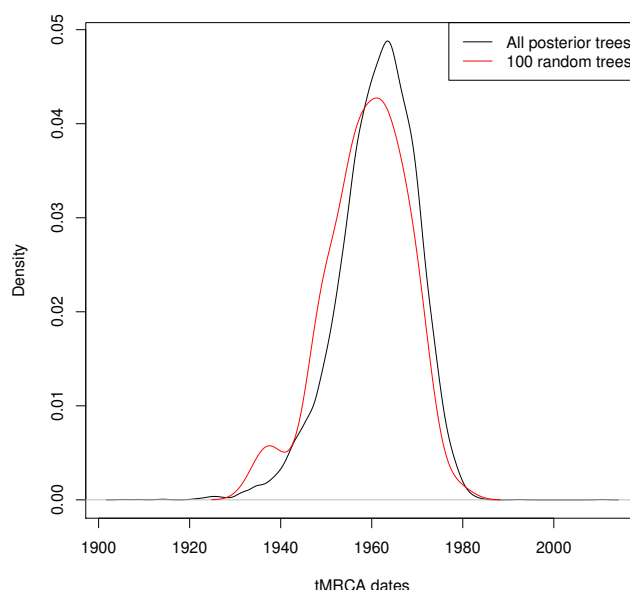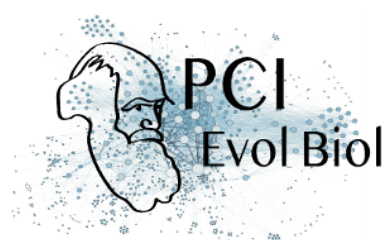
PCI Evol Biol

Figure S8. Density distributions of the t_{MRCA} for the observed Beast2 phylogeny (in black) and for the 100 phylogenies drawn at random in the posterior distributions of trees inferred by Beast2 (in red).
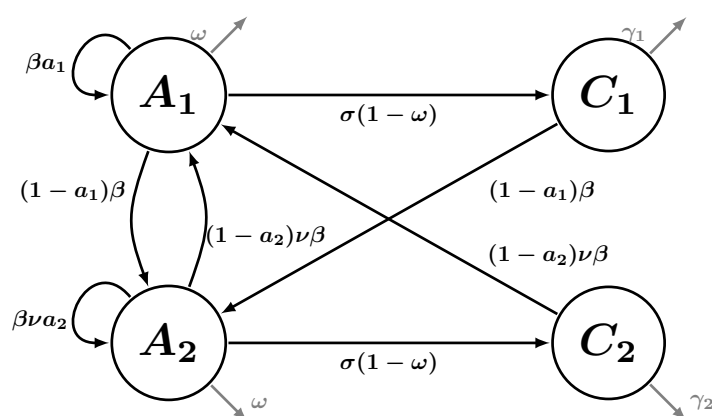
Figure S9. Diagram of the alternative model where all infected hosts first go through an acute phase (A_i) before recovering or progressing to the chronic phase (C_i). ω is the proportion of infections that clear before becoming chronic, σ is the rate at which acute infections become chronic, and other parameters are identical to those in the main text. The equations governing the dynamics of the system can be written as $\frac{dA_i}{dt} = a_i\beta_i(A_i + C_i) + (1-a_j)\beta_j(A_j + C_j) - \sigma A_i$ and $\frac{dC_i}{dt} = \sigma(1-\omega)A_i - \gamma_i C_i$ with $i \neq j$, $\beta_1 = \beta$ and $\beta_2 = \nu\beta$.